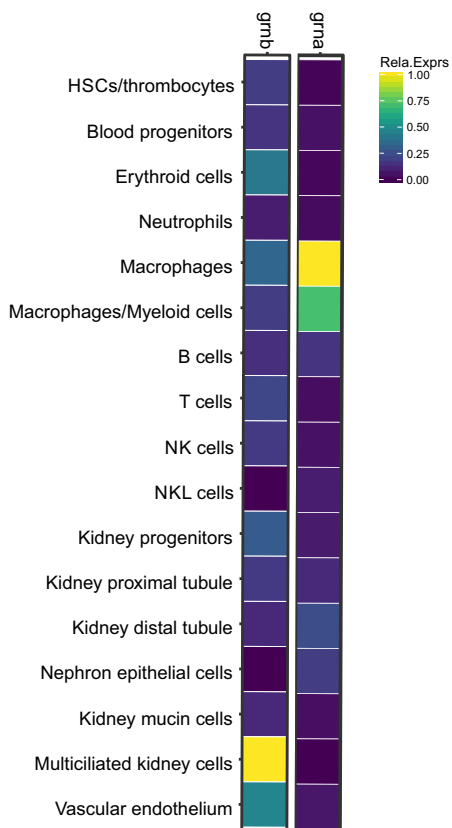
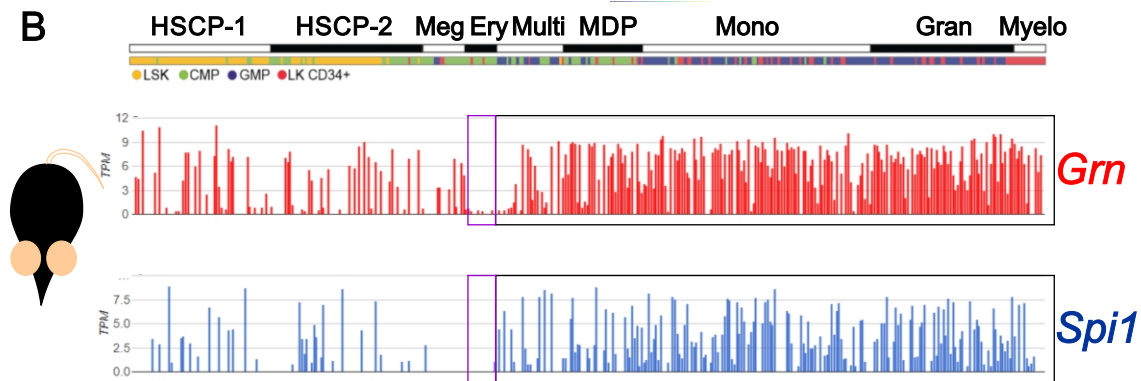


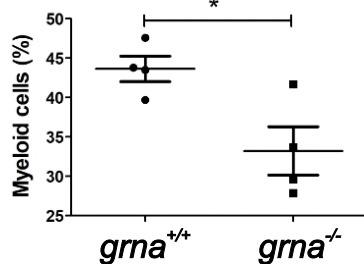
A



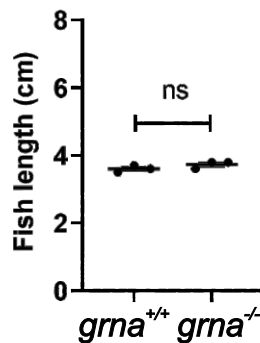
B

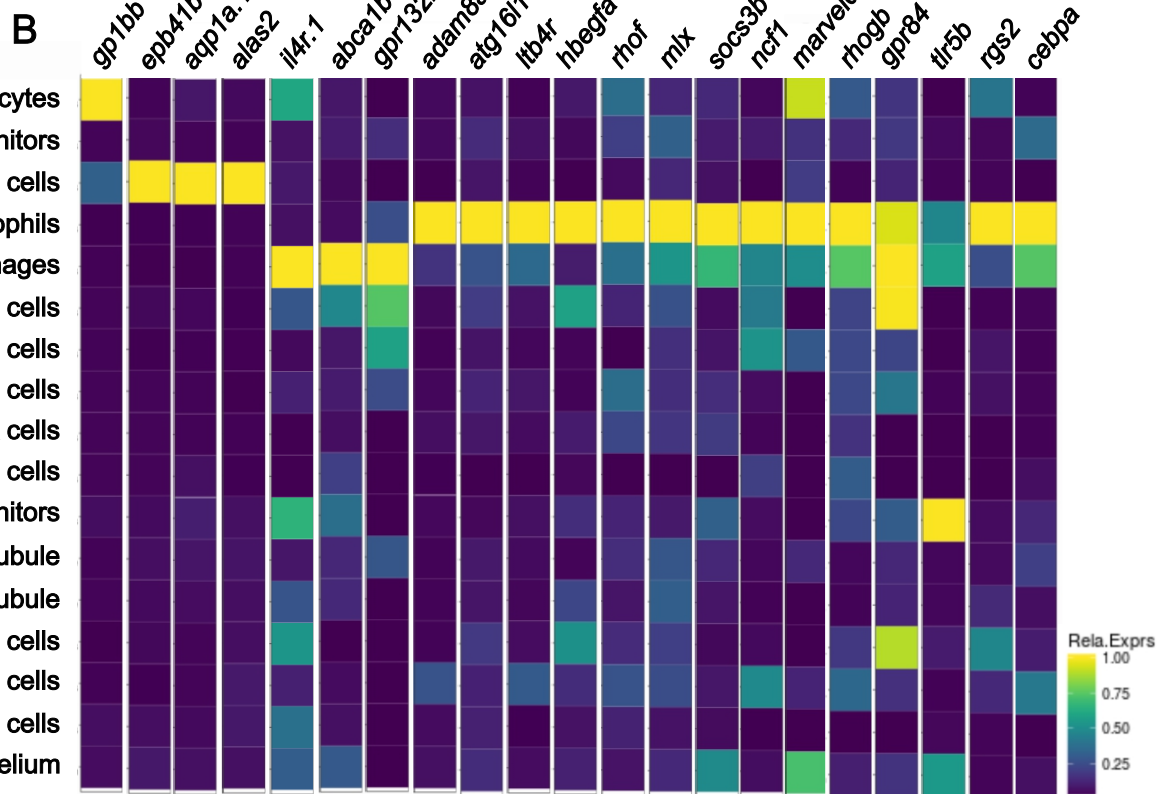
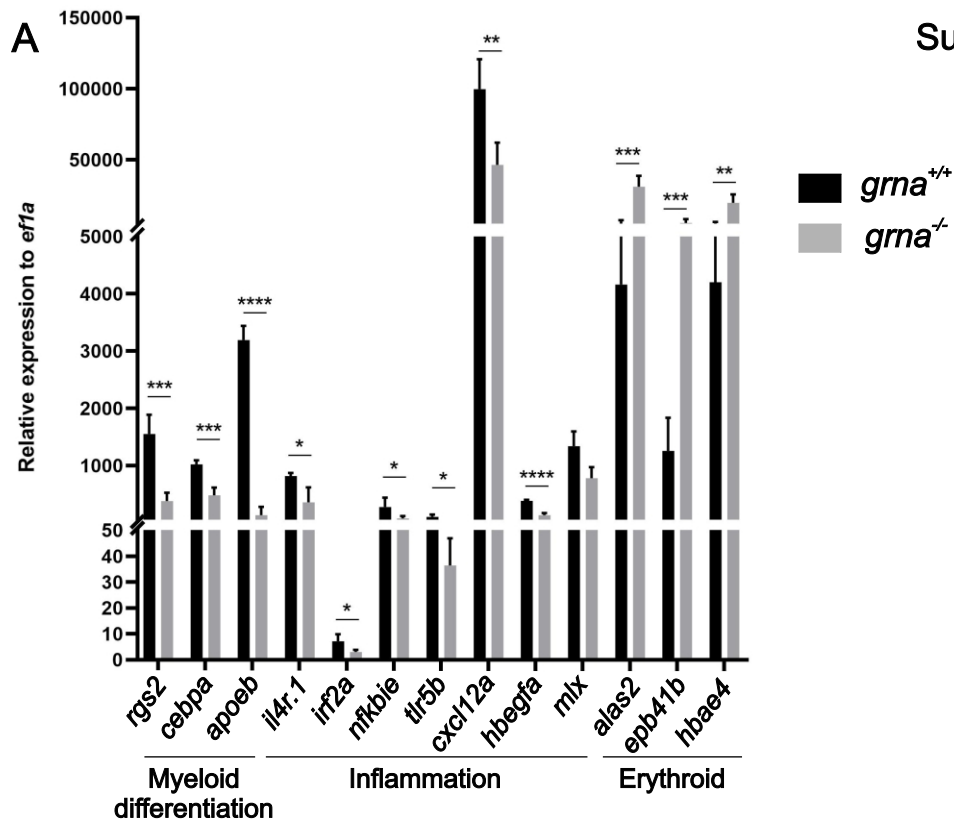


C

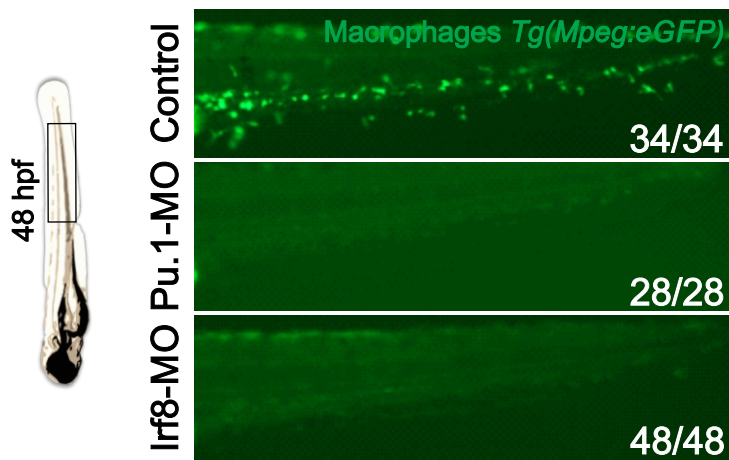


D

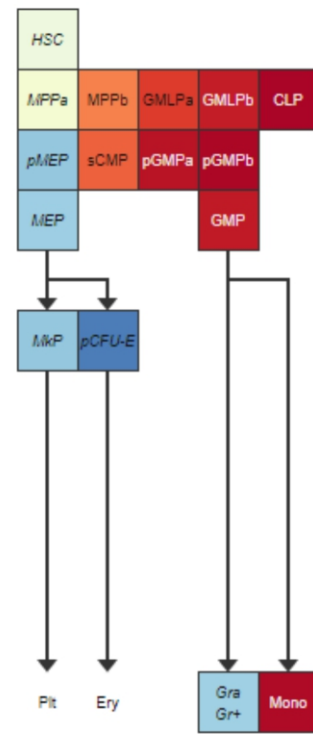
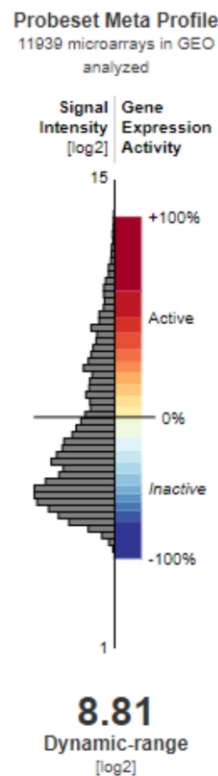




A



B

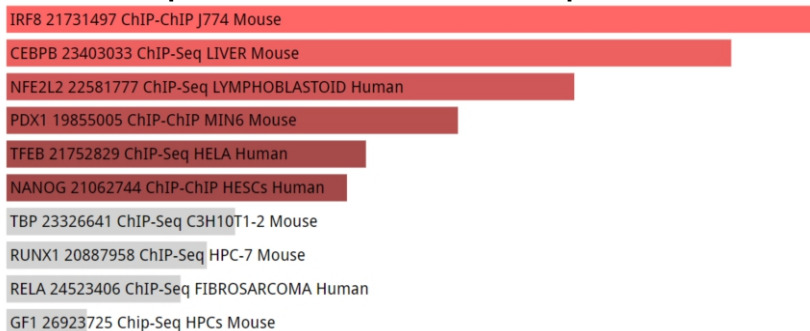


C

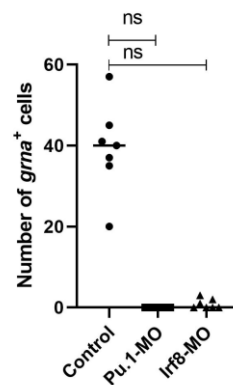


D

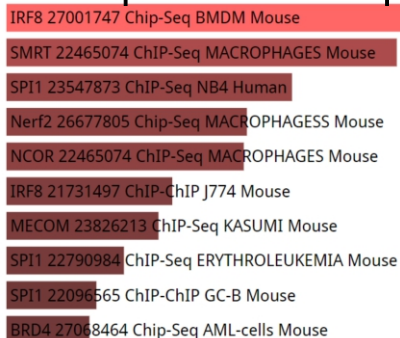
Transcription factors that bind *GRN* promoter



G



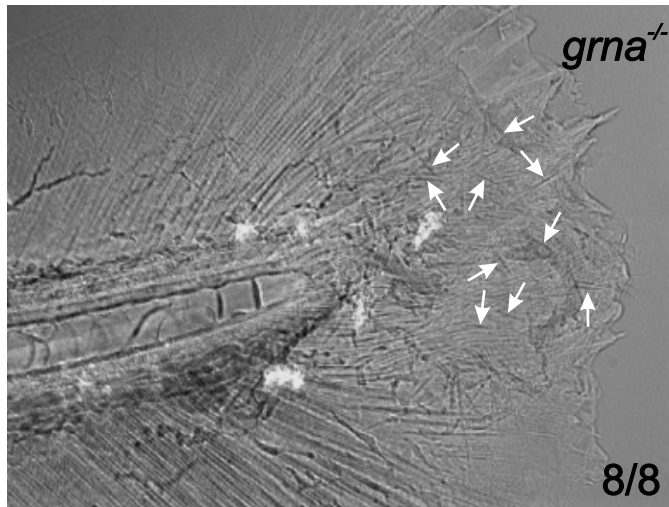
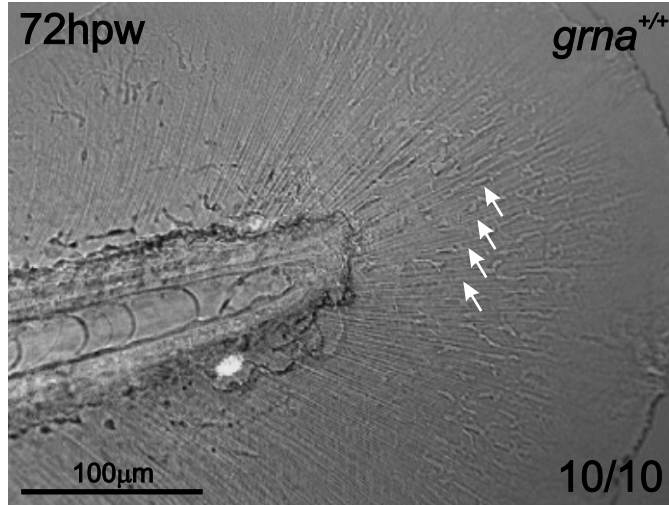
E Transcription factors co-expressed with *GRN*



F

Genes co-expressed with *GRN*

Gene Symbol	r	Pearson Correlation
CTSD		0.675
CD68		0.6584
MPEG1		0.6148
CTSB		0.6039
CTSA		0.5907
TREM2		0.5775
C3AR1		0.5674
CTSZ		0.564
LGALS3		0.554
LIPA		0.5415



Supplementary Figure 1: *grna* and *grnb* transcripts are ubiquitously expressed during early zebrafish embryonic development. WISH of 2, 6 and 10 hpf AB* zebrafish embryos hybridized with *grna* antisense and control sense probes (left panel), or *grnb* antisense and control sense probes (right panel). Numbers represent embryos with indicated expression.

Supplementary Figure 2: *grna* knockdown impairs macrophage development. (A-B) Schematic illustration of the *grna* and *grnb* knock-out and strategies. **(A)** Grna-MO1 and Grna-MO2 are 5'UTR-ATG translation blocking morpholinos. **(B-C)** Efficiency of splice-blocking MO against zebrafish *grnb*. RT-PCR analysis of WT and Grnb-MO injected embryos induced altered splicing of the *grnb* transcripts at 24 hpf. A 535 bp product containing 37 nucleotides insertion from *grnb* intron 5 (upper band) was detected in contrast to a 498 bp control (lower band in Grnb-MO injected embryos and WT control). This leads to an aberrant *grnb* mature mRNA with a shift in reading frame, which results in premature stop codons along the *grnb* mRNA. The annealing of MOs (green lines) and the inframe premature stop codons (arrowheads) are indicated. **(D)** Representative dots plots of 36hpf *Mpeg1.1:eGFP* embryos injected with mismatch, Grna-MO1 and Grna-MO2. **(E)** Quantification of Mpeg⁺ macrophages in Mismatch control n=4, Grna-MO1 n=4, and Grna-MO2, n=3 embryos. Each dot represents the percentage of Mpeg⁺ cells from the total events from 3 embryos. Horizontal lines and error bars indicate means \pm SEM (**p<0.01, ***p<0.001, ns: no significant). **(F-G)** Representative dot plot of intracellular flow cytometry using a specific antibody against the macrophage marker Mfap4 at 48 hpf *grna*^{+/+} (left) or *grna*^{-/-} embryos (right). Quantification shown in **(G)**. **(H)** WIHC for eGFP (green) and phospho-Histone 3 (Ser10) (red) in the caudal hematopoietic tissue of 36 hpf *Mpx:eGFP* embryos shows lack of colocalization between both markers. **(I-J)** Confocal images from 36 hpf *grna*^{-/-} or *grna*^{+/+} control embryos show incorporation of EdU (red) into the CHT between 26 and 36 hpf., Macrophages **(I)**

or neutrophils (**J**) are marked by immunofluorescence for Mfap4 or Mpx (green), respectively. White nuclei are stained with DAPI. White arrowheads represent macrophages (I) or neutrophils (J).

Supplementary Figure 3: Conserved gene expression levels among zebrafish *grna* and mouse *Grn* in hematopoietic cells. (A) Heat map derived from the online visualizer “Single Cell inDrops RNA-Seq Visualization of Adult Zebrafish Whole Kidney Marrow” (<https://molpath.shinyapps.io/zebrafishblood/#pltly>) (Tang *et al.*, 2017) for *grna* and *grnb* showing low or inexistent expression of *grnb* by kidney marrow hematopoietic cells and high expression by multiciliated kidney cells and vascular endothelium. In contrast, *grna* is highly expressed by macrophages and myeloid cells. (B) Gene expression levels in Transcripts Per Kilobase Million (TPM) for Granulin (*Grn*, red) and Pu.1 (*Spi1*, blue) from single cell RNA-seq data of mouse hematopoietic cells (Olsson *et al.*, 2016) showing high correlation between *Grn* and *Spi1* expression. (C) Quantification of the percentage of myeloid cells gated in Figure 3C in *grna*^{+/+} (n=4) and *grna*^{-/-} (n=4) zebrafish kidney marrows. (D) Quantification of zebrafish body length of *grna*^{-/-} and *grna*^{+/+} control siblings. Horizontal lines and error bars indicate means ± SEM. Ns, not significant; *p < 0.05. HSCP, Haematopoietic Stem Cell Progenitor; Meg, megakaryocytic; Ery, erythrocytic; Multi, Multi-lineage primed; MDP, monocyte-dendritic cell precursor; Mono, monocytic; Gran, granulocytic; Myelo, myelocyte (myelocytes and metamyelocytes).

Supplementary Figure 4: *Grna* depletion leads to decreased expression of myeloid specific genes and increased erythroid genes in the kidney marrow. (A) Kidney marrows were dissected from *grna*^{-/-} and control *grna*^{+/+} siblings and mRNA purified for qPCR. Levels of indicated transcripts along x-axis are shown relative to the housekeeping gene *ef1a*. Bars represent means ± S.E.M. of duplicate samples. (B) Heat map of the relative gene expression derived from

the online visualizer “Single Cell inDrops RNA-Seq Visualization of Adult Zebrafish Whole Kidney Marrow” (<https://molpath.shinyapps.io/zebrafishblood/#pltly>) (Tang *et al.*, 2017) of genes significantly enriched (A) or depleted (B) from RNA-seq of *grna*^{-/-} versus *grna*^{+/+} kidney marrows.

Supplementary Figure 5: Conserved regulatory expression of granulin in mammals and zebrafish. (A) *Mpeg1:eGFP* transgenic embryos were injected with control (Std), Pu.1, or Irf8 MOs and the tail region was visualized by fluorescence microscopy at 48 hpf. (B) Mouse hematopoietic model showing the dynamic expression of *Irf8* derived from microarray data (Affymetrix Mouse Genome 430 2.0 Array). Notice that lymphocyte differentiation beyond CLP is not shown here. (C) Screenshot of the regulatory feature of *ensembl.org* showing that PU.1 binds the *GRN* promoter in human hematopoietic cell lines based on epigenetic marks from experimental data available through *ensembl.org*. (D) Screenshot of mammalian granulin queried by ChEA showing the transcription factors whose peaks were detected at the granulin promoter. TFs were ranked based on p-value (red colors indicate p<0,05; gray colors indicate p>0,05). (E) Results from Harmonizome combined with ChEA showing the TFs that were co-expressed with the mammalian granulin. TFs were ranked based on p-value (red colors indicate p<0,05). (F) Screenshot of mammalian granulin queried by Harmonizome (<https://amp.pharm.mssm.edu/archs4/gene/GRN#correlation>) showing the first 10 most similar genes based on co-expression ranked by descendent Pearson correlation. HSC, Hematopoietic Stem Cell; MPP, Hematopoietic multipotential progenitors; GMLP, granulocyte–monocyte–lymphoid progenitor; CLP, common lymphoid progenitor; pMEP, pre of megakaryocyte-erythroid progenitor; MEP, megakaryocyte-erythroid progenitor; MkP, Megakaryocyte progenitor; PCFU-e, Colony Forming Unit-Erythroid; Plt, platelets; Ery, Erythrocytes; sCMP, strict common myeloid progenitor; pGMP, pre-granulocyte/macrophage; GMP, granulocyte/macrophage progenitors; Gra

Gr⁺, granulocytes; Mono, monocytes. **(G)** Quantification of *grna* expressing cells per embryo in the caudal hematopoietic tissue after pU.1 or Irf8 ablation using specific morpholinos (Figure 5B).

Supplementary Figure 6: Abnormal tissue repair in the absence of *grna*. Regenerated tail fins from *grna*^{+/+} and *grna*^{-/-} larvae at 72 hpw. Numbers represent larva with displayed phenotype.

Table S1

Gene or locus	Accession	Name	Nucleotide sequence (5'→3')	Use
<i>ef1a</i>	NM_131263.1	F	GAGAAGTTCGAGAAGGAAGC	q-PCR
		R	CGTAGTATTTGCTGGTCTCG	
<i>grna</i>	NM_001001949.3	F	AGCCAGACCTTCCCAAATCAT	
		R	CTCAGCAGGACAGGAAGAGC	
<i>grnb</i>	NM_212738.1	F	CGGCAAGAGTCTGGAAGAGT	
		R	CACACGGCCTTGACTAGAGG	
<i>grnb</i>	NM_130944.1	F2-MO	AAC TTTGTGCGACCTGGAAC	Morpholino validation
		R2-MO	TCTGGACAGCAGTGCTTTTG	
<i>grna</i>	NC_007114.7	pU.1-BS1-F	CACGAAAAGCCGA ACTCT	CUT&RUN-qPCR
		pU.1-BS1-R	GTTGGTCAGGCCTTTGAC	
<i>grna 5' enhancer</i>	NC_007114.7	pU.1-BS2-F	GCAGACAAAAGAGGAAAGAAGC	
		pU.1-BS2-R	ACAGAACAGATCCTGATG	
<i>grna 5' enhancer</i>	NC_007114.7	pU.1-BS3-F	GCAGATGATGATGTAAAAAAGGG	
		pU.1-BS3-R	CACATTTCTTTTACTTAACGC	
<i>grna</i>	NC_007114.7	Control-F	TGTCTTCTGATCTCAGTTCT	
		Control-R	GAGATAGACACGTACAGTTTG	
<i>grna 5' enhancer</i>	NC_007114.7	pU.1-BS5-F	GTTTCACGTAGCGGAAGC	
		pU.1-BS5-R	GGGTTGTGGCTGAAAAGG	
<i>grna</i>	NC_007114.7	pU.1-BS6-F	GCGAGTTTGAGCCACTTG	
		pU.1-BS6-R	CCTGATCACTTCCGGGAT	
<i>grna</i>	NC_007112.7	pU.1-BS7-F	CACTGCCAACTAGCGTTTC	
		pU.1-BS7-R	ACTGCATTAACACTTCCGA	
<i>rgs2</i>	NM_001002662.2	rgs2-qPCR-219-F	GTTGGCCTGTGAGGAGTTCAGA	Validation mRNAseq-qPCR
		rgs2-qPCR-219-R	TAGGAGTTGTGCTCCATCAGGT	
<i>cebpa</i>	NM_131885.2	cebpa -qPCR-165-F	CTCAGTGTCTAATTTCGTGCGAC	
		cebpa -qPCR-165-R	GATTCTGGTTTCCAGCTTACTC	
<i>apoeb</i>	NM_131098.2	Apoeb_qPCR_206bp_F	TGCAAGAGCTGAAGACCATGAT	
		Apoeb_qPCR_206bp_R	CTGGCTCATGTATGGCTGGAA	
<i>il4r.1</i>	NM_001013282.2	il4r.1-qPCR-F	TCCACAAAGGTGGCAAACAC	
		il4r.1-qPCR-R	GCGCTTACAATCCAGTGGTG	
<i>irf2a</i>	NM_001326712.1	irf2a -qPCR-F	TGAAAAAGCTGTTAGGAAAGGAAG	
		irf2a -qPCR-R	TGGTCATGCGTTCTACTTTTG	
<i>nfkbie</i>	NM_001080089.1	nfkbie-201_qPCR_199b_p_F	TCCAGGACCAGGATGGAAACA	

		nfkbie- 201_qPCR_199b p_R	TTCTTCATCAGCAGCCGCATGA
<i>tlr5b</i>	NM_001130595.2	tlr5b-qPCR-F	GATAGATGATCCGTGCTCACA
		tlr5b-qPCR-R	ACGACTTCAGTGTTTCAGGCA
<i>cxcl12a</i>	NM_178307.2	cxcl12a-qPCR- 175-F	ACCCAGAGACCAAATGGCTTCA
		cxcl12a-qPCR- 175-R	AGGTTAAGTGCTGGGTCAGCAA
<i>hbegfa</i>	NM_001111226.1	hbegfa- 002_qPCR_119b p_F	ACAAGGACTTTTGCATCCACG
		hbegfa- 002_qPCR_119b p_R	CTTCACCGGCAGAGAGAAATC
<i>mlx</i>	NM_001309416.1	mlx_qPCR_151b p_F	ACTCTCTGTTCCAGTCCTTCAG
		mlx_qPCR_151b p_R	AGTTGACCATTACCTGCTGC
<i>alas2</i>	NM_131682.2	alas2- 201_qPCR_150b p_F	CTTTAAGGAGAGCCCATCAGAG
		alas2- 201_qPCR_150b p_R	CCAACAGAATATCACACACCTCC
<i>epb41b</i>	NM_175084.2	epb41b- qPCR- 196-F	ATCCATTACGGTGGCAACACAC
		epb41b- qPCR- 196-R	CCTTCTTTCTTCCTCCAGTTTCC
<i>hbae4</i>	NM_001082834.1	hbae4-qPCR-F	TGCTCTCGAGTGCCGAAAA
		hbae4-qPCR-R	GGAACGTTGTGAACATCCTTAAAA

Table S2: List of genes down-regulated in *grna*^{-/-} versus *grna*^{+/+}

agpat4
larp6
zgc:153993
cebpa
far1
tpst1
arrb2a
zgc:66427
podxl
sepn1
f2r
grna
hk1
rbp5
cybrd1
sall1a
cxcl12a
amd1
trim8a
atg16l1
hbegfa
il13ra2
si:rp71-1g18.13
mlx
pitpnaa
cd81b
zgc:171579
si:dkey-20d21.12
slc16a3
ets1
slc35d1a
hsd3b7
dlc
syb1
papss2a
rhof
ltb4r
irf2a
ccdc149b
ncaldb
adam8a
hyal3
cers5
ncf1
enpp1
tlr5b
rbm48
pgp

zgc:55558
odc1
cd9b
wt1b
illr4
c6
mid1ip1b
ero1a
ippk
rhogb
rgs2
nfkbie
chsy3
mfsd2ab
agpat9l
rxrga
zgc:103510
soat1
plekhf1
nphs1
spry4
socs3b
efhd1
lima1a
cp
ahsg1
il13ra1
marveld1
lyve1a
ankrd37
lmo4b
zgc:77112
b3gnt5b
pigrl2.3
itgb3a
tank
abca1b
emilin1a
rpz3
zfand6
nphs2
gpr132b
cldn5b
prss35
gig2h
stab2
si:ch211-132b12.6
hnmt
si:ch211-264f5.2
gig2g
lpar5b

nr1h5
zgc:174888
dhrs3a
si:dkey-25e12.3
vtg7
ccl19a.1
si:dkey-61p9.11
gpr84
si:ch1073-67j19.1
scube1
foxd2
nfe2l1a
crfb17
htra3a
rspo1
coch
zgc:162952
zgc:92161
vtg1
tcf21
il4r.1
si:dkey-91m11.5
cyp1c2
m17
slc25a15a
zgc:152863
adra1bb
vtg4
rspo3
gig2j
si:ch73-86n18.1
sult5a1
zgc:158404
slc22a16
pltp
zgc:101699
cxcl8b.1
dio3b
vtg6
olfm2b
cyp26b1
serpine1
ugt5g1
sp5a
hamp
apoeb
cidec
dpep1
zgc:172053
g0s2
lgi2b

si:dkeyp-73d8.9
vtg3
tfa
f13a1a.1

Table S3: List of genes up-regulated in *grna*^{-/-} versus *grna*^{+/+}

zgc:172090
lmod2a
ddc
cyp7a1
frem2a
lgals2b
slc51a
slc25a38a
si:dkeyp-91i10.3
nsmfb
dio2
zgc:158427
mao
si:rp71-1f1.4
zgc:64106
zgc:77651
grm8b
alle
pcyt1ba
si:dkeyp-98a7.5
igfbp5a
csad
si:dkeyp-89c11.2
slc6a14
adrb2b
si:dkeyp-89c11.3
ela2l
si:ch211-197g15.10
unc119b
slco1f1
slc16a12b
irs2a
si:ch73-359m17.2
tal2
fbxo25
oxr1b
hsc70
zgc:86896
adrb3b
tnmem63bb
sox6
aadacl4
cnstb
aldh3a2b

slc52a3
gch2
krt15
ctsbb
tppp3
nt5c211
nad1.2
zgc:162780
dpysl3
fbxo32
slc6a13l
rhcgb
cdc25d
si:ch73-55i23.1
hexdc
mibp
tuba2
fam65c
nrp2b
creg1
harbi1
si:ch211-194e15.5
aplrb
rell2
zgc:198419
hif1a2
guca2b
adrb3a
adssl1
si:ch211-5k11.6
bag5
spns2
si:ch211-114i13.9
rnf183
si:dkey-58f10.11
suox
ank1a
ucp3
mfge8a
sstr5
dydc2
ascc1
cipca
slc25a39
3-Sep
fbxo3
jag1b
entpd8
epb41b
zgc:123107
si:dkey-58f10.10

zgc:194125
alas2
zgc:163057
hbp1
slc43a3a
zgc:172143
zgc:76872
p2rx3b
zgc:173915
zgc:153018
sdpra
sat1a.1
zgc:66440
gp1bb
tcp1112
aqp1a.1
slc12a3
ube2r2
dfna5b
fam46c
pip5k1bb

Table S4: List of genes down-regulated in *grna*^{-/-} versus *grna*^{+/+} expressed in myeloid cells

abca1b
adam8a
agpat4
agpat9l
amd1
apoeb
arrb2a
atg16l1
b3gnt5b
cebpa
cers5
cldn5b
cybrd1
cyp26b1
enpp1
far1
gig2h
gpr132b
gpr84
grna
hamp
hbegfa
hk1
hsd3b7
hyal3
il13ra1
il4r.1

irf2a
itgb3a
larp6
lima1a
ltb4r
marveld1
mid1ip1b
mlx
ncaldb
ncf1
nfkbie
odc1
papss2a
pgp
pitpnaa
plekhf1
rbp5
rgs2
rhof
rhogb
sall1a
serpine1
slc16a3
slc25a15a
slc35d1a
socs3b
spry4
stab2
sult5a1
sybl1
tfa
tlr5b
tpst1
cxcl12a
cp
podxl
dlc

Table S5: List of genes up-regulated in *grna*^{-/-} versus *grna*^{+/+} expressed in erythroid cells

ascc1
cipca
slc25a39
sep t3
fbxo3
jag1b
entpd8
epb41b
zgc:123107
si:dkey-58f10.10
zgc:194125

alas2
zgc:163057
hbp1
slc43a3a
zgc:172143
zgc:76872
p2rx3b
zgc:173915
zgc:153018
sdpra
sat1a.1
zgc:66440
gp1bb
tcp1112
aqpl1a.1
slc12a3

Extended materials and methods

Zebrafish husbandry and strains

Mutant *grna*^{*mde54a1*}, transgenic *Tg(mpx:eGFP)*^{*i114*}², *Tg(gata1:DsRed)*^{*sd2*}³, *Tg(mpeg1:eGFP)*^{*gl22*}⁴, *Tg(kdrl:HsHRAS-mCherry)*^{*s896*} (referred to as *kdrl:mCherry* throughout manuscript)⁵, *Tg(Lyz:Dsred2)*^{*nz50*}⁶, *Tg(Myf5:eGFP)*^{*zf42*}⁷, *Tg(LCR:eGFP)*^{*cz3325*}⁸ and various intercrosses of these lines were utilized.

Morpholino injection

Specific antisense morpholinos (MOs) (Gene Tools) were resuspended in water at 2mM. MOs used in this study were Standard-MO (Gene Tools), pu1-MO⁹, irf8-MO¹⁰, Grna-MO1 (also denoted as Grna-MO throughout the manuscript) 5'-TTGAGCAGGTGGATTTGTGAACAGC-3'¹¹, Grna control morpholino with 5 nucleotides mismatch 5'-TTGACCACGTGCATTTCTCAACAGC-3', Grna-MO2 5'-GGAAAGTAAATGATCAGTCCGTGGA-3'¹¹, and Grnb-MO 5'-CCACAGCGCAACTCTCACACCTG-3' (validated in this manuscript). Morpholinos were diluted in water at a concentration of 0.4 mM (Grna-MO), 0.4 mM (Grna mismatch-MO), 0.2 mM (Grna-MO2), 0.6 mM (Grnb-MO), 1.4 mM (irf8-MO) and 2 mM (pu1-MO) with phenol red solution and 2 nl were injected into the yolk ball of one-cell-stage embryos using a micromanipulator (Narishige) and PM 1000 cell microinjector (MDI). For Grnb-MO validation, 20 24 hpf zebrafish embryos injected with Grnb-MO or uninjected controls were collected and RNA was isolated with RNeasy (Qiagen), cDNA generated with qScript Supermix (Quanta BioSciences) and PCR performed with primers Grnb-F2-MO and Grnb-R2-MO (Table S1) for the detection of the wildtype (498 bp) or the mutant (535 bp) *grnb* amplicon. These amplicons were

sequenced. The mutant *grnb* amplicon contained 37 extra-nucleotides that changed the reading frame of the *grnb* mRNA.

Quantitative RT-PCR analysis

RNA was isolated from tissues with RNeasy (Qiagen), and cDNA generated with iScript gDNA Clear cDNA Synthesis Kit (BioRad). Primers to detect zebrafish transcripts are described in Table S1. qPCR was performed in CFX real-time PCR detection system (BioRad), and relative expression levels of genes were calculated by the following formula: Relative expression = $2^{-(Ct[\text{gene of interest}] - Ct[\text{housekeeping gene}])}$.

Flow cytometry

To quantify the myeloid fraction in kidney marrows from *grna*^{-/-} and *grna*^{+/+} control siblings, adult zebrafish between three to nine months old were anesthetized in tricaine, subjected to cardiocentesis and kidney dissection as previously described³. The resulting kidney suspension was gently triturated with a P1000 pipette and filtered with a 30µm cell strainer (Thermo Fisher Scientific, NC9084441) and stained with Sytox Red (Life Technologies) to exclude dead cells. Flow cytometric acquisitions were performed on a LSR-Fortessa (BD) and analyses were performed using FlowJo software (v10.3, Tree Star) as previously described³.

To analyze macrophage numbers in Grna morphants, three 48 hpf *Mpeg1:eGFP*⁺ embryos per replicate (three to four replicates per experiment) previously injected with Grna-MO1, Grna-MO2 or Grna mismatch MO were dechorionated with pronase (Roche) and anesthetized in tricaine. Gently triturated with a P1000 pipette and chemically dissociated with liberase TM (Roche) for 20 minutes in agitation. The resulting cell suspension was filtered and stained with Sytox Red to exclude dead cells. Flow cytometric acquisitions were performed on a FACS LSR-

Fortessa (Becton Dickinson) and analyses were performed using FlowJo software (v10.3, Tree Star).

For intracellular flow cytometry, flow cytometry was performed on a LSR Fortessa (BD) and data were analyzed using FlowJo software (v10.3, Tree Star). Following dissociation of 48 hpf *grna*^{+/+} and *grna*^{-/-} embryos (three embryos per condition) with liberase TM (Roche) as described below, cells were fixed with PFA 4% and permeabilized for 30 minutes on ice with PBS containing 0.1% triton. Intracellular staining was performed with anti zebrafish mfap4 antibody (Gentex, GTX132692), dilution 1:250, followed by staining with 5ug/ml of goat anti-rabbit IgG (H+L) antibody, alexa-488 (Thermo Fisher, A11034).

To isolate embryonic cells by FACS (*Fluorescence-activated cell sorting*) for qPCR analysis, approximately 200 16 hpf *Myf5:eGFP*⁺; 22 hpf *Kdr11:mCherry*⁺, *Gata1:Dsred*⁻; 48 hpf *Mpx:eGFP*; 48 *Mpeg1:eGFP*; or 36 hpf *LCR:eGFP* embryos were dechorionated with pronase (Roche) and anesthetized in tricaine. Gently triturated with a P1000 pipette. The resulting cell suspension was filtered and stained with Sytox Red to exclude dead cells. Cell sorting of positive fluorescent cells was performed with a FACS ARIAI (Becton Dickinson).

In Situ Hybridization

Reagents used for FISH: TSA Plus Cyanine 3/Fluorescein system (NEL753001KT), anti-Digoxigenin-POD, Fab fragments (11207733910), and anti-fluorescein-POD, Fab (11426346910). Embryos were analyzed using a Sp5 confocal (Leica). Embryos were imaged using a Leica M165C stereomicroscope equipped with a DFC295 color digital camera (Leica) and FireCam software (Leica) for WISH, and Sp5 confocal (Leica) for FISH.

Whole-mount immunohistochemistry, EdU incorporation assay and TUNEL

The following antibodies were used: rabbit anti-phospho-Histone H3 (Ser10) antibody (Millipore, 06-570) (dilution 1:100), anti-GFP antibody chicken IgY (Aves Labs GFP-1020) (dilution 1:500), goat anti-Chicken IgY (H+L) Alexa-488 (Thermofisher A-11039) (dilution 1:500), donkey anti-rabbit IgG (H+L) Alexa-594 (Thermofisher A21207) (dilution 1:500). The samples were imaged with a Leica Sp5 confocal.

Our EdU incorporation assay was adapted from a previously described protocol¹²: Mutant and wild-type siblings were injected pericardially with 1 nl EdU solution (200 μ M EdU, 2% DMSO, 0.1% phenol red) at 24 hpf, followed by fixation at 36 hpf. Whole-mount immunostaining was adapted from a previously described protocol¹³, followed by Click-iT detection as per manufacturer's guidelines (Invitrogen, C10340). Antibodies used include rabbit polyclonal anti-Mfap4 (1:100; GTX132692) or rabbit anti-Mpx (1:100, GTX128379), followed with Alexa Flour 488 goat anti-rabbit (1:200, A-21206) and DAPI (1:500, Invitrogen; D1306). Imaging of the CHT was performed with a Zeiss LSM 700 confocal microscope with Zen9 software and images were processed with ImageJ.

The TUNEL assay was performed as previously described¹³ with the following modification: Streptavidin-Alexa647 (Jackson Laboratories; 016-600-084) was used for the detection of apoptotic cells.

Fin amputation and enumeration of myeloid cells

48hpf zebrafish embryos were anesthetized with tricaine and a single cut traversing the entire dorsoventral length of the caudal fin was made using a surgical scalpel size #15 (19-200-218, fisher scientific). Embryos were individually isolated and imaged at each given timepoint. Throughout the time course, the initial amputation plane of each embryo was determined by superimposing the

image captured at each timepoint with the image of the initial cut using Adobe Photoshop CS6. The caudal-most tip of notochord was used as a landmark for spatial alignment. Quantification of regenerate area was determined using ImageJ.

Animals were subjected to WISH for *pu.1* (myeloid progenitors), *mfap4* (macrophages), or *mpx* (neutrophils) at 48 hpf at varying locations (tail or head, listed in figures) and cells expressing the above mentioned transcripts were imaged and manually counted per individual. To image and enumerate macrophages *in vivo* after tail resection, fluorescence microscopy was performed on *Mpeg1:eGFP* transgenic animals. Z-sections of the tail region were captured using Leica Thunder imager with DFC9000 GT camera and LAS X navigator, and manually counted.

Cytology

Cytospin preparations were made with 1×10^5 to 2×10^5 kidney cells cytocentrifuged at 300 rpm for 5 min onto glass slides in a Thermo Scientific Shandon CytoSpin 4. Cytospin preparations were processed through Wright-Giemsa stains (Fisher Scientific, 5029782) for morphological analyses and differential cell counts. Briefly: Wright Stain Solution was placed upon the smear for 2 mins and washed with distilled water. Subsequently, the slides were placed for 10 minutes in a coplin jar containing Giemsa and rinsed with distilled water.

Morphological analyses and differential cell counts of kidney marrow hematopoietic cells

200 non-erythroid nucleated differential cell counts were assessed in *grna*^{-/-} or *grna*^{+/+} kidneys after cardiocentesis, kidney dissection, cytospin and staining with Wright-Giemsa. The morphological features to identify each cell type are the following. Early myeloid precursors, round to ovoid in shape with a round to ovoid-shaped pink nucleus. Chromatin pattern finely granular and semi frequently with distinct round nucleoli. High nuclei to cytoplasmic (N:C) ratio

with a moderate amount of deep blue cytoplasm. Late myeloid precursors (immature neutrophils): round to ovoid to bilobed nuclei are with light purple to darker pink coloration. Slightly clumped chromatin pattern and no distinct nucleoli. Moderate N:C ratio with a blue to light blue cytoplasm. Neutrophils (mature): smaller in size than late myeloid precursors. Round to ovoid to bilobed to segmented dark purple nucleus smaller than late myeloid precursors. Moderate N:C ratio with a light blue cytoplasm and often bubbly vacuolated appearance. Macrophages: round to ovoid in shape. Nuclear shapes included round, ovoid, bilobed, and lobulated forms that have a pale pink to purple coloration. The chromatin pattern is finely stippled that occasionally has distinct nucleoli. Moderate N:C ratio that is moderately high with a blue appearance frequently vacuolated and sometimes contained melanin pigment. Lymphocytes: small round to ovoid-shaped cells. Round to ovoid-shaped nucleus, coarsely clumped chromatin pattern, and no distinct nucleoli. High N:C ratio with a scant amount of pale blue cytoplasm.

Peripheral blood collection and hematocrit determination

Adult (6-11 months old) *grna*^{-/-} and *grna*^{+/+} control siblings were subjected to cardiocentesis for blood collection. Briefly, adult zebrafish were treated with a solution containing the anesthetic Tricaine (3-aminobenzoic acid ethyl ester; Sigma A-5040) at a concentration of 160-200mg/L for 2 minutes. Then, cardiac puncture was performed with a heparinized P10 pipette for PB collection. 4-10 μ l of PB per fish were deposited on a slide, and microcapillary tubes (Sigma-Aldrich, P1924-1PAK) were placed on top to collect the blood by capillarity. The tubes were sealed with critoseal (McCormick scientific, 215003), and the samples were placed on ice until analyzed as followed. The microcapillary tubes were centrifuged for three minutes in a microhematocrit centrifuge at 13.3 RPM (Sorvall Legend Micro 17). The hematocrit was evaluated using a microcapillary tube

reader (IEC International) by a board-certified clinical pathologist. Markedly hemolyzed samples were rejected.

CUT&RUN

Adult wild type AB* zebrafish between three to nine months old were anesthetized in tricaine, subjected to cardiocentesis and kidney dissection as previously described³. The resulting kidney suspension was gently triturated with a P1000 pipette and filtered with a 30µm cell strainer (Thermo Fisher Scientific, NC9084441). 90,000 -120,000 cells were used per condition to perform CUT&RUN using CUT&RUN assay kit (86652S, Cell signaling) with an anti zebrafish Pu.1 antibody (GTX128266, GeneTex) (4 µl) or rabbit (DA1E) IgG Isotype control antibody (as recommended in kit protocol) following the manufacturer instructions with the following modifications: Digitonin dilution 5:1000. Incubation time for primary antibody: 10 hours at +4°C; for pAGMase: 1 hour at +4°C. Digestion time: 30 min.

To identify potential binding sites for Pu.1 in the promoter and enhancer regions of *grna*, the entire *grna* gene sequence plus 10Kb 5' upstream *grna* were subjected to Pu.1 binding sites prediction using Consite (<http://consite.genereg.net/>) and Tomtom (<http://meme-suite.org/tools/tomtom>). The transcription factor binding profile matrix for Pu.1 ID: MA0080.4 from JASPAR was utilized when using Tomtom, and user defined profile (<http://jaspar.genereg.net/matrix/MA0080.4/>) and 70% identity analyses were used for Consite. The fragment located at +23765 from the *grna* ATG start codon was used as a control, since it lacked any predicted binding sites for Pu.1.

RNA sequencing

Adult *grna*^{-/-} and *grna*^{+/+} control fish (three fish per condition) were subjected to cardiocentesis and kidney dissection as described here. RNA was isolated with RNeasy (Qiagen) following the

manufacturer instructions. Total RNA was assessed for quality using an Agilent TapeStation 4200, and samples with an RNA Integrity Number (RIN) greater than 8.0 were used to generate RNA sequencing libraries using the TruSeq Stranded mRNA Sample Prep (Illumina, San Diego, CA). Samples were processed following manufacturer's instructions, starting with 50 ng of RNA and modifying RNA shear time to five minutes. Resulting libraries were multiplexed and sequenced with 75 basepair (bp) single reads (SR75) to a depth of approximately 20 million reads per sample on an Illumina HiSeq 4000. Samples were demultiplexed using bcl2fastq v2.20 Conversion Software (Illumina, San Diego, CA).

RNA-seq data was mapped to Reference Consortium Zebrafish Build 10 (UCSC Genome GRC10/danRer10; Sept 2014) using Olego¹⁴ and normalized using standard analysis pipelines such as cufflinks¹⁵⁻¹⁷. featureCounts¹⁸ from subread package is used to compute the raw read counts for each gene. TPM (Transcripts Per Millions)^{19,20} values were computed from the raw read counts using a custom perl script and $\log_2(\text{TPM}+1)$ is used to compute the final log-reduced expression values. DESeq2 1.26.0²¹ R package is used to compute differentially expressed genes at 1% false discovery rate. Volcano plot and heatmap were created using python matplotlib package (version 2.1.1).

Statistical analysis

Data were analyzed by unpaired T-test in GraphPad Prism 8. In all figures, solid red bars denote the mean, and error bars represent S.E.M. * $p < 0.05$, ** $p < 0.01$, *** $p < 0.001$, **** $p < 0.0001$, n.s. not significant, n.d. not detected.

References

1. Solchenberger B, Russell C, Kremmer E, Haass C, Schmid B. Granulin knock out zebrafish lack frontotemporal lobar degeneration and neuronal ceroid lipofuscinosis pathology. *PLoS One*. 2015;10(3):e0118956.
2. Renshaw SA, Loynes CA, Trushell DM, Elworthy S, Ingham PW, Whyte MK. A transgenic zebrafish model of neutrophilic inflammation. *Blood*. 2006;108(13):3976-3978.
3. Traver D, Paw BH, Poss KD, Penberthy WT, Lin S, Zon LI. Transplantation and in vivo imaging of multilineage engraftment in zebrafish bloodless mutants. *Nat Immunol*. 2003;4(12):1238-1246.
4. Ellett F, Pase L, Hayman JW, Andrianopoulos A, Lieschke GJ. mpeg1 promoter transgenes direct macrophage-lineage expression in zebrafish. *Blood*. 2011;117(4):e49-56.
5. Bertrand JY, Chi NC, Santoso B, Teng S, Stainier DY, Traver D. Haematopoietic stem cells derive directly from aortic endothelium during development. *Nature*. 2010;464(7285):108-111.
6. Hall C, Flores MV, Storm T, Crosier K, Crosier P. The zebrafish lysozyme C promoter drives myeloid-specific expression in transgenic fish. *BMC Dev Biol*. 2007;7:42.
7. Chen YH, Wang YH, Chang MY, et al. Multiple upstream modules regulate zebrafish myf5 expression. *BMC Dev Biol*. 2007;7:1.
8. Ganis JJ, Hsia N, Trompouki E, et al. Zebrafish globin switching occurs in two developmental stages and is controlled by the LCR. *Dev Biol*. 2012;366(2):185-194.
9. Rhodes J, Hagen A, Hsu K, et al. Interplay of pu.1 and gata1 determines myelo-erythroid progenitor cell fate in zebrafish. *Dev Cell*. 2005;8(1):97-108.
10. Li L, Jin H, Xu J, Shi Y, Wen Z. Irf8 regulates macrophage versus neutrophil fate during zebrafish primitive myelopoiesis. *Blood*. 2011;117(4):1359-1369.
11. Li YH, Chen MH, Gong HY, et al. Progranulin A-mediated MET signaling is essential for liver morphogenesis in zebrafish. *J Biol Chem*. 2010;285(52):41001-41009.
12. Sidhwani P, Leerberg DM, Boezio GLM, et al. Cardiac function modulates endocardial cell dynamics to shape the cardiac outflow tract. *Development*. 2020;147(12).
13. Espin R, Roca FJ, Candel S, et al. TNF receptors regulate vascular homeostasis in zebrafish through a caspase-8, caspase-2 and P53 apoptotic program that bypasses caspase-3. *Dis Model Mech*. 2013;6:383-396.
14. Wu J, Anczukow O, Krainer AR, Zhang MQ, Zhang C. OLEgo: fast and sensitive mapping of spliced mRNA-Seq reads using small seeds. *Nucleic Acids Res*. 2013;41(10):5149-5163.
15. Trapnell C, Pachter L, Salzberg SL. TopHat: discovering splice junctions with RNA-Seq. *Bioinformatics*. 2009;25(9):1105-1111.
16. Trapnell C, Roberts A, Goff L, et al. Differential gene and transcript expression analysis of RNA-seq experiments with TopHat and Cufflinks. *Nat Protoc*. 2012;7(3):562-578.
17. Trapnell C, Williams BA, Pertea G, et al. Transcript assembly and quantification by RNA-Seq reveals unannotated transcripts and isoform switching during cell differentiation. *Nat Biotechnol*. 2010;28(5):511-515.
18. Liao Y, Smyth GK, Shi W. featureCounts: an efficient general purpose program for assigning sequence reads to genomic features. *Bioinformatics*. 2014;30(7):923-930.
19. Li B, Dewey CN. RSEM: accurate transcript quantification from RNA-Seq data with or without a reference genome. *BMC Bioinformatics*. 2011;12:323.
20. Pachter L. Models for transcript quantification from RNA-Seq. *arXiv*. 2011;1104.3889.
21. Love MI, Huber W, Anders S. Moderated estimation of fold change and dispersion for RNA-seq data with DESeq2. *Genome Biol*. 2014;15(12):550.